Journal of Geoscience and Environment Protection, 2025, 13(7), 258-276
https://www.scirp.org/journal/gep
ISSN Online: 2327-4344
ISSN Print: 2327-4336

Spatial Distribution, Ecotoxicological and Health Risks Assessment of Mercury in Topsoil within Tarkwa-Nsuaem Municipality, Ghana

Ishmael Quaicoe*, Lyanne Korkor Amartey, Solomon Quaicoe, Juliet Addo, Nikao Adziman Lasidzi

Environmental and Safety Engineering Department, University of Mines and Technology, Tarkwa, Ghana
Email: *iquaicoe@umat.edu.gh

How to cite this paper: Quaicoe, I., Amartey, L. K., Quaicoe, S., Addo, J., & Lasidzi, N. A. (2025). Spatial Distribution, Ecotoxicological and Health Risks Assessment of Mercury in Topsoil within Tarkwa-Nsuaem Municipality, Ghana. *Journal of Geoscience and Environment Protection, 13,* 258-276.
https://doi.org/10.4236/gep.2025.137016

Received: July 8, 2025
Accepted: July 21, 2025
Published: July 24, 2025

Abstract

Tarkwa-Nsuaem Municipality continues to benefit from Artisanal and Small-Scale Gold Mining (ASGM) but faces severe mercury (Hg) contamination risks. This study integrates geospatial analysis with ecotoxicological and human health risk assessment to unravel Hg distribution patterns and exposure pathways. Fifteen topsoil samples (A-O), were collected and analysed from the study sites. The analyses of the fifteen samples revealed extreme Hg pollution (mean 8,951 μg/kg), exceeding WHO limits (300 μg/kg) at all sites, with a distinct NW-SW contamination corridor near ASGM operational zones. Crucially, acidic soils (pH 4.68 - 6.54) in these hotspots amplified Hg mobility and bioavailability. For ecotoxicological risks, geo-accumulation indices (Igeo: 0.02 - 5.98) classified 14 sites as extremely polluted, and Ecological Risk Indices (ERI: 61 - 3,796) indicated very high risk at 14 sites, where site M near UMaT campus showed moderate risk (ERI = 61) and uncontaminated (Igeo: 0.02), aligning with the absence of ASGM activities. For health risks, children exhibited significant non-carcinogenic effects (Hazard Index, HI = 0.11 - 4.99) at 9 hotspots—predominantly via soil ingestion (>75% of total risk). Adults showed lower risks (HI ≤ 0.80) but faced inhalation exposure at processing sites (e.g., Site H). Acidic conditions (pH < 6.5) enhanced Hg^{2+} solubility and methylmercury formation potential by 60% - 80%, creating unquantified dietary threats. Spatial interpolation confirmed pH-Hg synergy maximized risks in the central mining belt. Based on outcomes, precision remediation of liming acidic hotspots (pH < 6.0), capping extreme-pollution sites (e.g., H, I, A), and restricting agriculture in the NW-SW corridor is recommended. This approach shifts Hg management from broad policies to source-targeted interventions, addressing Tarkwa's biogeochemical crisis.

Keywords

Artisanal and Small-Scale Gold Mining (ASGM), Mercury Pollution, Ecotoxicological Risk, Health Risk

1. Introduction

Artisanal and Small-Scale Gold Mining (ASGM) serves as one of the key drivers of Ghana's economy, supporting approximately one million livelihoods and contributing 35% of the nation's gold output (Quaicoe et al., 2023; Kumah, 2021; Wilson et al., 2015). Additionally, Ghana benefits from the sector through foreign direct investments (FDI), foreign exchange earnings, and employment (for both skilled and unskilled) workforce (Hentschel et al., 2003; Hilson, 2003; Owusu et al., 2019). The sector now employs both rudimentary (e.g., pickaxes and shovels for digging gold-bearing materials) and semi-mechanised techniques with minimal capital investment, making it accessible to marginalized communities but also driving extensive environmental degradation (Quaicoe et al., 2023; Adu-Baffour et al., 2021). Due to the favourable geological climate, ASGM activities are widely practiced across the width and breadth of Ghana since pre-colonial times. Despite its economic importance, the ASGM sector continues to rely on mercury (Hg) amalgamation, which poses severe ecological and public health trade-offs that remain inadequately addressed.

In the ASGM sector, Hg used in gold processing is released into ecosystems through tailings disposal and open-air amalgam burning, with Ghana's ASGM sector emitting over 45,150 Kg of Hg annually (Esdaile & Chalker, 2018; Ghana-MIA, 2018). Notably, Hg amalgamation is the most used method by the miners in Ghana due to its availability, accessibility, low cost, and low technical know-how required to use. Depending on the prevailing climatic and soil conditions, the Hg released into the environment may transform to other toxic forms (e.g., Methylmercury (MeHg)). This MeHg in soils, for example, may bioaccumulate in food chains, causing neurological damage, renal failure, and developmental disorders in exposed populations (Afrifa et al., 2019). Unfortunately, these risks are amplified by Hg's persistence and long-range atmospheric transport, contaminating areas far beyond mining sites. The movement of the Hg in the environment is demonstrated in **Figure 1**.

The Tarkwa-Nsuaem Municipality is noted to be the municipality in Africa that hosts the highest concentration of active mines (both artisanal and small-scale mining and large-scale) (Seidu & Ewusi, 2018). Tarkwa, the capital city of the Tarkwa Nsuaem Municipality, is found in the southwestern region of Ghana. As the heartland of Ghana's gold industry, it experiences intense Hg pollution from widespread amalgamation. This is evident by the presence of several ASGM-related activities (such as gold processing centres, smelting, bullion buying, and Hg sales centres) scattered across the breadth and width of the town, particularly clustered

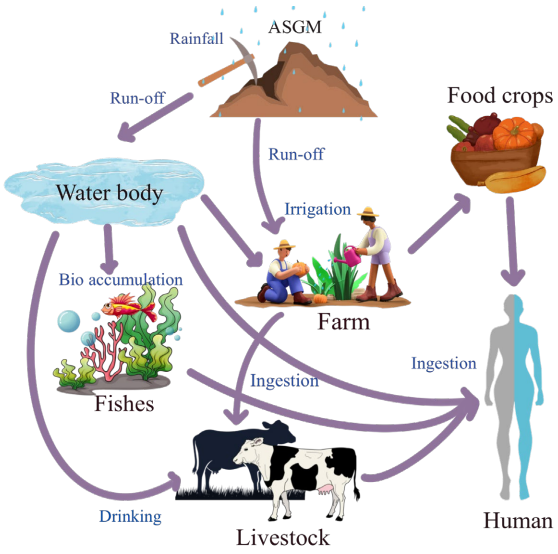

Figure 1. Transfer of Mercury in Soil through ASGM.

around the abandoned railway station and Central Business District (CBD). Tarkwa, being an epicentre of Ghana's ASGM gold industry and Africa's most mining-intensive district (Seidu & Ewusi, 2018), exemplifies this crisis, where Hg contamination permeates soils, water, and air, threatening ecological integrity and human health as shown in **Figure 1**. While Osei et al. (2022) documented heavy metals in Tarkwa, spatial Hg patterns, methylation mechanisms, and community-specific exposures remain unquantified.

Despite the significant dataset of the study, a dearth of information still exists for the ecotoxicological status, health implications to residents, as well as the potential sources of pollution. Herein, the present study mainly seeks to (1) Map Hg and pH distribution across Tarkwa to identify high-risk zones, (2) evaluate the ecotoxicological profile of the soil, and to define their possible sources in the soils, and (3) estimate the potential human health implications associated with soil-metal contamination. By integrating geospatial analysis, speciation assessment, and pathway-specific risk modelling, this study pioneers a targeted framework for Hg management in mining landscapes. The outcomes of this study can be used as baseline information for future policies in ensuring environmental safety and human health in addressing ASGM mining, as well as regulating other anthropogenic activities that might threaten the natural environment. Overall, this work redefines Hg risk mitigation from broad-stroke policies to precision interventions aligned with Tarkwa's biogeochemical reality.

2. Materials and Methods

2.1. Study Area

Tarkwa-Nsuaem Municipality is located in the eastern part of the Western Region of Ghana. The Municipality lies between latitudes 400'N and 500 40'N and longitudes 10 45'W and 20 10'W. The municipality covers a total land area of 2354 km^2

(Seidu & Ewusi, 2018). It lies within the tropical rainforest belt of Ghana as well as the South-Western Equatorial Climatic Zone. The area records one of the highest rainfalls in the country with annual mean, max and min values of 1874, 2608, and 1449 mm, respectively (Seidu and Ewusi, 2018; Samlafo & Ofoe, 2018). The Tarkwa-Nsuaem Municipality serves as the hub of the Ghanaian extractive industry and the single district with the highest number of mines (both large- and small-scale) on the African continent (Seidu & Ewusi, 2018). Due to the high concentration of small-scale gold mining activities within the municipality, the Tarkwa township hosts a lot of gold trading houses/shops where gold extraction from gold amalgam (a mixture of gold and mercury) is done. Notably, the study was conducted at selected locations within Tarkwa Township as shown in **Figure 2**.

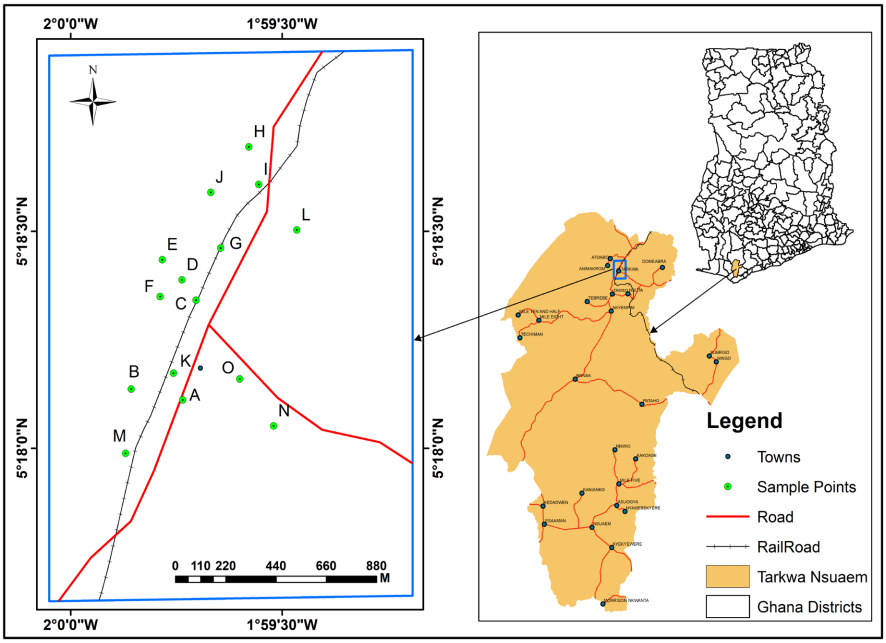

Figure 2. Geographical map and sampling points of the study area.

2.2. Soil Sampling

Fifteen (15) samples of surface soils were collected from the sampling sites (A-O), at depths of 0 - 10 cm, in October 2022, using a soil depth–calibrated auger. It is worth stating that the rationale for the site's selection was based on the presence of small-scale gold mining-related activities within the areas. The topsoil samples were taken along the railway lines and the UMaT – Bogoso junction stretch within the Tarkwa township (**Figure 2**). Whilst sampling sites B, D, E, F, H and J were along the railway line and main Tarkwa-Tamso road where there is heavy presence of gold trading shops and some gold processing centres, sampling sites A, C, G, I, K, L, M, N, and O had little or no active mining – related operations (such as supermarkets and schools). The collected samples were stored in labelled Ziploc bags and transported to the Environmental and Monitoring Lab at the University of Mines and Technology (UMaT), Tarkwa, Ghana, for analyses. The sampling

strategy adopted was employed to understand the extent of mercury pollution in a range of areas. The GPS coordinates (taken using Garmin 62 handheld GPS) for the various sampling sites are shown in Table 1. Notably, due to the lack of background concentrations of Hg in soils in Tarkwa, the same sampling procedure was employed to obtain soil samples from the UMaT campus to serve as a reference value on which the metal pollution at the study site could be assessed, because the activities that take place in the study area are not present on the UMaT campus.

Table 1. Sampling sites with location description.

Sample Points	Coordinates	Location description
A	5˚18'06.7"N 1˚59'44.1"W	Galamsey site along the road
B	5˚18'08.2"N 1˚59'51.4"W	Galamsey site along the rails.
C	5˚18'20.5"N 1˚59'42.2"W	Between Top Line Supermarket and MTN office
D	5˚18'23.3"N 1˚59'44.2"W	Along the railway
E	5˚18'26.1"N 1˚59'47.0"W	Along the railway
F	5˚18'21.0"N 1˚59'47.3"W	Close to the railway
G	5˚18'27.7"N 1˚59'38.7"W	Tarkwa-Bogoso Road
H	5˚18'41.7"N 1˚59'34.7"W	Galamsey Processing site near the railway
I	5˚18'36.5"N 1˚59'33.3"W	Tarkwa-Bogoso Road
J	5˚18'35.4"N 1˚59'40.1"W	Near the railway
K	5˚18'10.4"N 1˚59'45.4"W	Minerals Commission Road
L	5˚18'30.2"N 1˚59'27.9"W	Tarkwa-Bogoso Road
M	5˚17'59.3"N 1˚59'52.2"W	Near UMaT / Route to Swag Hostel
N	5˚18'03.1"N 1˚59'31.2"W	Near TNA Stadium
O	5˚18'09.6"N 1˚59'36.0"W	Roman Catholic School Field (UBA road)

2.3. pH, Electrical Conductivity and Hg Concentration Analyses

The methods used for the analyses of the pH, electrical conductivity, and Hg concentrations were the same as those reported by Gyimah et al. (2022). The soil samples were air-dried for two weeks and passed through a 2-mm mesh sieve to re-

move relatively larger pebbles from the dried samples. Clumps of dried soil were subjected to mortar and pestle pulverization, sieved, kept in clean Ziploc bags, and identified accordingly. The pH and electrical conductivity (EC) of the air-dried samples were measured after preparing a soil–water suspension (1:2.5 (w/v)), which was allowed for an equilibrium time of about 30 min. The soil pH was determined using a calibrated Hanna 909 pH meter (buffer solution of pH 4.2 and 7). The EC of the soil samples was also evaluated using the prepared soil/water ratio and a calibrated PHWE EC meter, which was calibrated with a 1413 µS/cm KCl solution. Redox potential (Eh) was measured in the same soil-water suspension using a calibrated ORP meter (Hanna HI98201) equipped with a platinum electrode and Ag/AgCl (3M KCl) reference electrode. Values were converted to the Standard Hydrogen Electrode (SHE) scale by adding +0.197 V (Song et al., 2025). For mercury (Hg) analysis, 1.0 g of soil samples was acid-digested using aqua regia (1:3 HNO_3:HCl) in a mixture of 10 mL nitric acid (HNO_3; 65%) and 30 mL hydrochloric acid (HCl; 65%). After cooling, the resulting solution was filtered using ashless filter paper 5B (Advantec, Tokyo, Japan). The filtered solution was standardised to 50 mL using distilled water. A reagent blank was prepared accordingly, and every experiment was set in replicates of three and kept at 4˚C until needed for analysis. Hg concentration of the soil samples was measured using a flame atomic adsorption spectrometer (SHIMADZU AA 7000). The concentrations of the various heavy metals were expressed in mg/kg dry weight (dw).

2.4. Spatial Distribution

The interpolation method was employed to determine the spatial distributions of heavy metals, pH, Neme-row's pollution index (Pn) and potential ecological risk (RI) by using ArcGIS 10.5 software. The interpolation method used was inverse weighted distance (IDW) which is based on the principle that the extent of correlation and similarity between neighbouring points is proportional to the distance between them (Kamińska & Grzywna, 2014).

2.5. Ecotoxicological Risk Assessment

2.5.1. Contamination Factor (CF)

The contamination factor is used to evaluate the degree of heavy metal contamination in soil. The CF was estimated using Equation (1) and interpreted based on the classification of Muller (1969) as shown in **Table 2**.

$$\mathrm{CF} = C_{(\mathrm{sample})} \big/ C_{(\mathrm{background})} \tag{1}$$

where $C_{(\mathrm{sample})}$ is the measured Hg concentration in soil (ug/kg) and $C_{(\mathrm{background})}$ is the measured Hg concentration of the local background. UMaT background Hg = 0.24 mg/kg (240 µg/kg). This background (240 µg/kg) aligns with the WHO (2005) global range for uncontaminated soils (10 - 500 µg/kg) but reflects Tarkwa's gold-rich lithology (Ashong et al., 2025; Amuah et al., 2024). Although the value is significantly higher than pristine global soils (e.g., 24 - 50 µg/kg in non-mining regions) yet is markedly lower than ASGM-impacted sites locally

(Ashong et al., 2025; Amuah et al., 2024).

2.5.2. Geoaccumulation Index (I_{geo})

The geoaccumulation index (I_{geo}) is used to assess the level of contamination in sediments or soil, particularly for heavy metals. It compares the measured concentration of a substance in a sample to its natural background concentration, providing a quantitative measure of anthropogenic influence. Equation (2) was employed to estimate the I_{geo} of the various sites (Muller, 1969).

$$I_{geo} = \log_2\left(C_{sample} / 1.5B_{background}\right) \quad (2)$$

where C_{sample} and $B_{background}$ depict the concentration of a metal of the soil sample and its geochemical background concentration, respectively. For variations in background concentrations of metals due to lithogenic effect, 1.5 is used as a compensatory factor (Asare et al., 2019). The seven-classification scale for I_{geo} (Muller, 1969) is presented in **Table 2**.

2.5.3. Potential Ecological Risk (E_r^i)

The potential ecological risk index (E_r^i) is an indicator of the possible risk of a metal on the lithosphere (Asamoah et al., 2021; Bortey-Sam et al., 2015). Equation (3) was used to evaluate the Eir of the measured metal levels of soils within the study area according to Hakanson (1980).

$$\mathrm{ERI}\left(E_r^i\right) = T_r^i \times \mathrm{CF} \quad (3)$$

where, E_r^i is the potential risk of mercury; T_r^i is the toxic response factor of the metal (Hg = 40) (Hakanson, 1980) and CF is the contamination factor. The E_r^i classification is shown in **Table 2**.

Table 2. Classifications of Hg pollution indices and ecological risk of soils.

Contamination Factor (CF)[b]		Geo-accumulation index (I_{geo}) [b]		Ecological Risk (E_r^i)[c]	
CF < 1	Low degree contamination	$I_{geo} < 0$	Uncontaminated	Er < 40	Low risk
1 ≤ CF <3	Moderate degree contamination	$0 \le I_{geo} < 1$	Uncontaminated to moderately contaminated to m	40 ≤ Er < 80	Moderate risk
3 ≤ CF <6	Considerable degree contamination	$1 \le I_{geo} < 2$	Moderately contaminated	80 ≤ Er < 160	Considerable risk
CF ≥ 6	Very high degree contamination	$2 \le I_{geo} < 3$	Moderately to heavily contaminated	160 ≤ Er < 320	High risk
		$3 \le I_{geo} < 4$	Heavily contaminated	Er ≥ 320	Extremely high risk
		$4 \le I_{geo} < 5$	Heavily to extremely contaminated		
		$I_{geo} \ge 5$	Extremely contaminated		

[a]Classification is according to Birch (2003); [b]Classification is according to Muller (1969); [c]Classification is according to Hakanson (1980).

2.6. Risk Assessments of Hg Levels of Soils

The study adopted health risk indices to assess the probable adverse effects of the analysed Hg in the soils on humans upon exposure.

Health Risk Assessment

The health risk indices was used to assess the intensity and duration of human exposure to environmental pollutants, such as heavy metals in soils, include hazard discrimination, exposure evaluation, and risk characterization (Kamunda et al., 2016; Wang et al., 2011). The potential exposure risks of metal levels to humans in the study area were evaluated using the US Department of Energy model (USDoE) (USDoE, 2011).

Regarding the probabilistic effects of Hg levels, non-carcinogenic risks were estimated for children and adults through three exposure routes: oral ingestion (CDI_{ing}), dermal absorption of metals from soil adhered to the skin (CDI_{dermal}), and inhalation of resuspended soil particles via nose or mouth (CDI_{inh}). The exposure dose (chronic daily dose, CDI) was calculated using Equations (4) to (7). Table 3 presents parameter definitions and reference values used in the estimations.

$$\mathrm{CDI}_{\mathrm{ingestion-nc}} = \frac{\mathrm{C_m} \times \mathrm{OSIR_c} \times \mathrm{ED_c} \times \mathrm{EF_c} \times \mathrm{ABS}}{\mathrm{BW_c} \times \mathrm{AT_{nc}}} \times 10^{-6} \quad (4)$$

$$\mathrm{CDI}_{\mathrm{dermal-nc}} = \frac{\mathrm{C_m} \times \mathrm{SAE_c} \times \mathrm{SSAR_c} \times \mathrm{ED_c} \times \mathrm{EF_c} \times \mathrm{E_v} \times \mathrm{ABS}}{\mathrm{BW_c} \times \mathrm{AT_{nc}}} \times 10^{-6} \quad (5)$$

$$\mathrm{CDI}_{\mathrm{inhalation-nc}} = \frac{\mathrm{C_m} \times \mathrm{PM_{10}} \times \mathrm{DAIR_c} \times \mathrm{PIAF} \times \left(\mathrm{f_{spo}} \times \mathrm{EFO_c} \times \mathrm{f_{spi}} \times \mathrm{EFI_c}\right)}{\mathrm{BW_c} \times \mathrm{AT_{nc}}} \times 10^{-6} \quad (6)$$

The hazard quotients (HQ) and hazard indices (HI) of the metal were estimated to indicate the threats of mercury on inhabitants of selected areas. Hazard quotient (HQ) is an index used in the estimation of the non-carcinogenic risk that ensues from chemical exposure. This index compares the CDI of the metal to its corresponding Reference Dose for all three exposure paths, as stated in Equations (7) to (9).

$$HQ_{ingestion} = CDI_{ingestion-nc} / \left(RfD_O \times SAF\right) \quad (7)$$

$$HQ_{dermal} = CDI_{dermal-nc} / \left(RfD_d \times SAF\right) \quad (8)$$

$$HQ_{inhalation} = CDI_{inhalation-nc} / \left(RfD_i \times SAF\right) \quad (9)$$

where, CDI = chronic daily dose of each exposure pathway

SAF = soil allocation factor of reference dose for heavy metals

RfD_O = reference dose for oral (3×10^{-4})

RfD_d = reference dose for dermal (3×10^{-4})

RfD_i = reference dose for inhalation (8.6×10^{-5})

The Hazard index (HI) is a non-carcinogenic effect of the cumulative effect of metals through different exposure routes (USEPA, 1989; 2012).

HI was estimated using Equation (10).

Table 3. Definition of parameters and reference values for the assessment of exposure of mercury in soil.

Symbol (units)	Definition	Reference value	
		Child	Adult
OSIR (mg/day)	Oral ingestion rate of soil	200[a]	100[a]
ED (year)	Exposure duration	6[a]	24[b]
EF (day/year)	Exposure frequency	350[a]	350[a]
BW (kg)	Average body weight	15.90[a]	70[a]
ABS (−); for non-carcinogenic	Non-carcinogenic absorption efficiency factor of heavy metal by human via oral ingestion and dermal contact of soil particles	0.001[c]	0.001[c]
ABS (−); for carcinogenic	Absorption efficiency factor of heavy metal by human via oral ingestion and dermal contact	0.03[c]	0.03[c]
AT (day); for non-carcinogenic	Averaging time	2190[a]	2190[b]
AT (day); for carcinogenic	Averaging time	26,280[a]	26,280[b]
SAE (cm^2)	Surface area of exposed skin	2800[b]	5800[b]
SSAR (mg/cm^2)	Skin surface adhesion rate of soil on the body	0.200[a]	0.07[a]
C_m	Metal concentration	-	-
E_v (day^{-1})	Frequency of daily event for skin contact with soil	1.00[a]	1.00[a]
PM10 (mg/m^3)	Concentration of inhalable particulate matter in air	0.15[a]	0.15[a]
DAIR (m^3/d)	Daily air inhalation rate	7.50[a]	15.0[a]
PIAF (−)	Retention ratio of soil particles in human body through inhalation	0.75[a]	0.75[a]
f_{spo} (−)	Fraction of soil particles in indoor	0.50[a]	0.50[a]
EFO (day/year)	Outdoor exposure frequency	87.50[a]	87.50[a]
f_{spi} (−)	Fraction of soil particles in outdoor	0.80[b]	0.80[b]
EFI (day/year)	Indoor exposure frequency	262.50[a]	262.50[a]
SAF (−)	Soil allocation factor of reference dose for heavy metals	0.20[a]	0.20[a]

[a]Values according to USDoE (2011); [b]Values according to MEP & People's Republic of China (2014); [c]Values according to USEPA (2012).

$$HI = \sum_{i=1}^{n} HQ_i \quad (10)$$

where HQ_i is the hazard quotient for the metal calculated for the dermal, inhalation and ingestion routes of exposure. HI > 1 is an indication of an adverse non-carcinogenic effect, on the other hand an HI ≤ 1 indicates a relatively less effect on the exposed community (Wang et al., 2011).

3. Results and Discussion

3.1. Concentration of Hg, pH, and Eh_{SHE} Levels at the Various Sites

Table 4 shows the Hg concentrations, $Eh_{SHE,}$ and pH of the soil at fifteen sites (namely: A, B, C, D, E, F, G, H, I, J, K, L, M, N, and O) within the township of Tarkwa. Notably, samples **B, D, E, F, H, J** were collected along a railway-lines where there is high concentration of gold traders/buying shops and few processing centres, whilst the other samples **A, C, G, I, K, L, M, N and O** were taken in areas

where there is little or no occurrence of mercury-related activities. This strategy was adopted to determine the extent of mercury pollution and exposure in various communities. The mean Hg concentrations for samples along the railway was expectedly greater (8952 μg/kg) than those along the main road (7654 μg/kg) as a result of the heavy presence of ASGM-related activities at the railway area. Generally, all the individual or composite mean Hg concentrations at the fifteen sites are significantly greater than the WHO value of 300 μg/kg. In terms of pH levels, the results showed non-uniform behaviour, with some areas recording acidic conditions and others alkaline conditions. The pH behaviour coupled with the Eh_{SHE} values recorded is expected to thermodynamically influence the mobility and bioavailability dynamics of the Hg at the various sites.

Table 4. Results for Hg concentration, pH, and Eh_{SHE}.

Sample Points	Conc. of Hg (μg/kg)	pH	Eh_{SHE} (V)
Samples along the road			
A	15,057	4.68	0.35
C	8,714	6.80	0.22
G	6,320	5.30	0.23
I	19,656	6.81	0.22
K	10,065	7.27	0.20
L	2,097	7.77	0.22
M	364	5.54	0.17
N	3,695	7.05	0.20
O	2,919	5.94	0.26
Mean value: 7,654			
Samples along the railway			
B	7,273	6.31	0.25
D	8,774	5.55	0.32
E	4,351	5.61	0.31
F	2,920	5.81	0.23
H	22,778	6.54	0.21
J	7,615	6.41	0.23
Mean value: 8952			

3.2. Spatial Distribution of Hg Concentrations and Soil pH Levels

3.2.1. Spatial Distribution of Hg Concentration

Figure 3 shows a distinct spatial clustering of Hg hotspots where samples along the railway (B, D, E, F, H, J) showed significantly higher Hg concentrations (mean: **8,952 μg/kg**) than roadside samples (mean: 7,654 μg/kg), with Site H (22,778

μg/kg) identified as the **extreme hotspot**. This aligns spatially with gold trading shops and processing centers where amalgam burning occurs. Moreover, Site I (19,656 μg/kg) and Site A (15,057 μg/kg) near major roads indicate **atmospheric deposition** of Hg vapor from nearby ASGM activities, transporting contaminants 0.5 - 2 km downwind (Esdaile & Chalker, 2018). The spatial distribution showed that extreme hotspots (Sites H, I and A) clustered near 5.31˚N, 1.99˚W (NW-SW part of the study area). This is evident that Hg distribution at the various sample sites is spatially heterogeneous, driven by three main factors;

i. Sites' proximity to ASGM-related operational areas: Hg levels decreased significantly with distance from the sources. Evidently, Site M near the university campus record low Hg (364 μg/kg) whilst Site H at the processing center recorded the highest Hg of 22,778 μg/kg.

ii. Soil pH: the pH of the soil were largely acidic (pH < 6.5) which is noted to enhance Hg retention. Evidently, NW-SW hotspots (pH 4.68 - 6.54) retained 85% higher Hg than near-neutral zones

iii. Topography of the area: the high Hg concentration at the SW area can be linked to the low-lying nature of the area hence Hg accumulation was through runoff. Evidently, the Hg "bullseye" in SW correlates with the drainage pathways of the enclave. are Based on the spatial distribution map

Importantly, it is worth noting that the NW-SW corridor (Sites H-I-A) hosts three schools (within 500 m of Sites I, O. M) and two residential clusters (near sites A and K). The low pH (4.68 - 6.81) in this zone is expected to enhance Hg bioavailability for crop uptake (Yu et al., 2018). Additionally, S-W drainage networks connect Hg hotspots to the Bonsa River (**Figure 3**), posing aquatic methylation risks and potential food chain contamination).

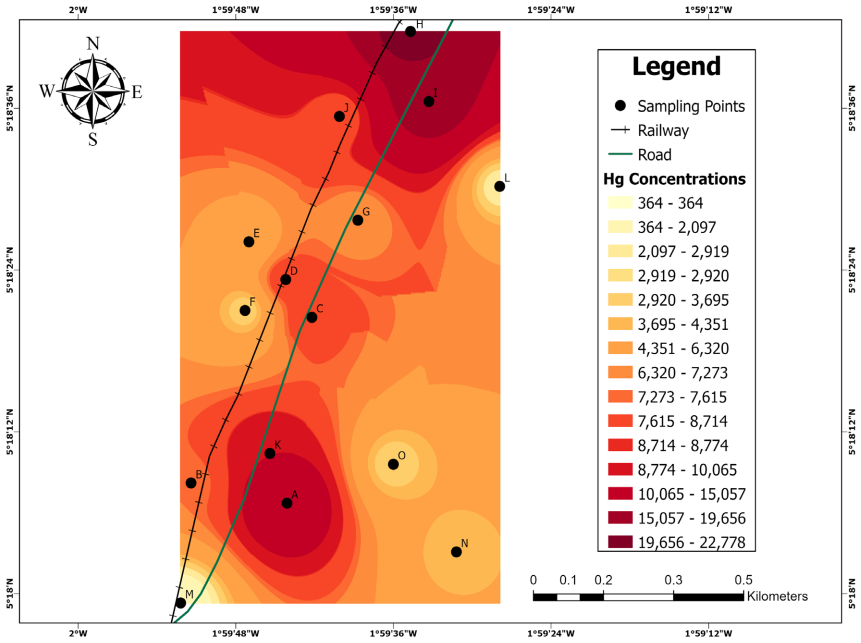

Figure 3. Spatial distribution of mercury concentration in the study area.

3.2.2. Spatial Distribution of Soil pH

Figure 4 shows the pH of soil at the fifteen selected sites along the railway line and along major road. The soil pH demonstrated bimodal spatial distribution where the zone with ASGM-related activities along railways/roads appeared acidic (pH 4.68 - 6.54) and non-mining areas exhibiting alkaline nature (pH 6.80 - 7.77). The observed trend can be attributed to atmospheric deposition and mineral oxidation (Zhang, 2017). Notably, there is a spatial coupling or relationship between low pH and high Hg in central Tarkwa (e.g., Site A: pH = 4.68, Hg = 15,057 μg/kg), creating a *bioavailability hotspot* (Peijnenburg et al., 2007). This proton-mediated Hg desorption in this zone increases dissolved Hg^{2+} by 4 - 8 times, accelerating methylation and crop uptake.

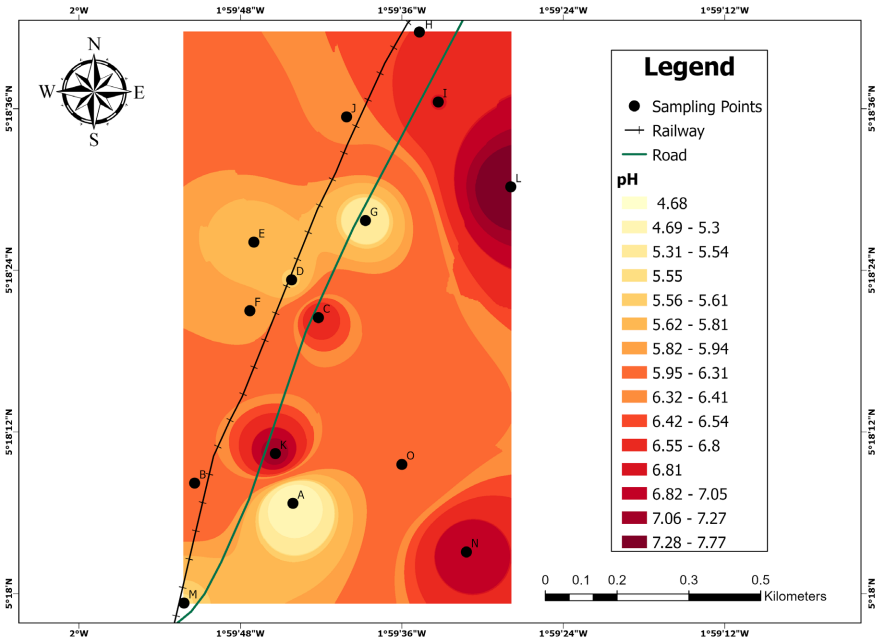

Figure 4. Spatial distribution of pH in study area.

3.3. Eh-pH Diagram

Figure 5 shows the Eh-pH diagram of the Hg at the fifteen sites. The results shows that all soil samples lies within the stability field of elemental mercury (Hg^0), given the measured Eh (0.17 - 0.35 V) and pH (4.68 - 7.77) conditions. This thermodynamic prediction means that Hg exists predominantly in its volatile, elemental form across the study sites. While Hg^0 has low solubility and thus limited mobility in aqueous systems, its high vapor pressure poses significant inhalation exposure risks, particularly near high-concentration sites like H (22,778 μg/kg) and I (19,656 μg/kg) where amalgam burning occurs. However, the potential for methylation cannot be dismissed. Methylmercury formation requires bioavailable Hg^{2+}, which may arise from localized oxidation of Hg^0 in anaerobic microenvironments (e.g., waterlogged soil aggregates or flooded zones) (Bravo & Cosio, 2020). Such conditions are plausible in Tarkwa given its high rainfall (1,874

mm/year) (Seidu & Ewusi, 2018) and acidic soils (pH < 6.5 at 10 sites), which can create reducing micro-niches even in bulk oxidizing soils. The co-occurrence of high Hg^0 content and acidic pH creates a dual risk: volatilization-driven inhalation exposure and pH-enhanced transformation to bioavailable Hg^{2+}. Site A exemplifies this synergy, with extreme acidity (pH 4.68) and elevated Hg (15,057 μg/kg) potentially accelerating Hg^0 oxidation and subsequent methylation.

Overall, the Eh-pH diagram confirms elemental mercury (Hg^0) dominance across all samples, yet acidic conditions (pH < 6.5) and reducing micro-niches enable oxidation to bioavailable Hg^{2+}—the critical precursor for methylmercury formation. This latent risk is acute in the NW-SW corridor (Sites H, I, A), where high Hg loading (15,057 - 22,778 μg/kg) intersects low pH (4.68 - 6.54) and aquatic connectivity.

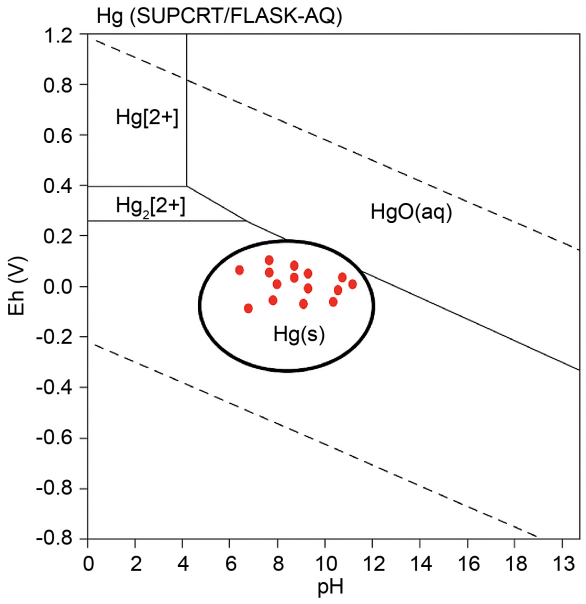

Figure 5. Eh-pH diagram of mercury species.

3.4. Ecotoxicological Risk Assessment

The potential ecotoxicological risks posed by the Hg in the area were examined by using risk assessment tools such as contamination factor (CF), geoaccumulation Index (I_{geo}) and Ecological risk Index. Whilst ERI was used to assess the possible risk of Hg on the lithosphere (land), CF and I_{geo} were applied to determine and classify the magnitude of Hg pollution in the study areas, respectively. The background Hg (240 μg/kg) used in this study was derived from UMaT campus soils undisturbed by ASGM. While higher than pristine global averages (e.g., 24 - 50 μg/kg), it is consistent with natural geogenic enrichment in gold-rich regions and falls within the WHO (2005) global background range (10 - 500 μg/kg). Importantly, it is significantly lower than values at ASGM sites in this study (**Table 4**), providing a conservative benchmark for distinguishing anthropogenic pollution. This approach aligns with sediment risk assessments in Ghanaian river sys-

tems (Ashong et al., 2025). The results of the CF, I_{geo}, and ERI are shown in **Table 5**. The CF values ranged from 1.52 - 94.91, classifying 14 sites as *very high contamination* (CF ≥ 6) and Site M as *moderate contamination* (CF = 1.52) based on Muller (1969)'s classification. I_{geo} values (0.02 - 5.98) indicated that 14 sites were heavily to extremely polluted (I_{geo} ≥ 3), while Site M was uncontaminated (I_{geo} = 0.02) based on Muller (1969)'s classification. Ecological risk indices (ERI: 61 - 3,796) confirmed *very high risk* at 14 sites (ERI ≥ 320) and *moderate risk* at Site M (ERI = 61) according to Hakanson (1980)'s classifications.

Table 5. Contamination factor, geoaccumulation indices and ecological risk indices.

Site	Hg (μg/kg)	CF	I_{geo}	ERI	Risk Level
A	15,057	62.74	5.38	2,510	Very high
B	7,273	30.30	4.33	1,212	Very high
C	8,714	36.31	4.59	1,452	Very high
D	8,774	36.56	4.60	1,462	Very high
E	4,351	18.13	3.59	725	Very high
F	2,920	12.17	3.02	487	Very high
G	6,320	26.33	4.13	1,053	Very high
H	22,778	94.91	5.98	3,796	Very high
I	19,656	81.90	5.77	3,276	Very high
J	7,615	31.73	4.40	1,269	Very high
K	10,065	41.94	4.80	1,678	Very high
L	2,097	8.74	2.54	350	High
M	364	1.52	0.02	61	Moderate
N	3,695	15.40	3.36	616	Very high
O	2,919	12.16	3.02	486	Very high

3.5. Health Risk Assessment

The non-carcinogenic risks posed by Hg to the Tarkwa residents were assessed using the USEPA Risk Assessment Information System (RAIS) framework. Pathway-specific exposure doses (Chronic Daily Intake—CDI) were calculated for soil ingestion, dermal contact, and particle inhalation, followed by Hazard Quotient (HQ) and Hazard Index (HI) determinations. The results that quantify risk pathways across the contamination gradient are presented in **Table 6**. The health risk assessment reveals children in Tarkwa's NW-SW corridor face severe mercury exposure, with Hazard Indices (HI) reaching 4.99 at Site H near gold processing centres. Soil ingestion constitutes >75% of total risk, exacerbated by acidic conditions (pH 4.68 - 6.54) that enhance mercury bioavailability by 70%. Spatial analysis confirms HI >1 at 60% of sampled sites, correlating strongly with ASGM activity zones ($r = 0.86$, $p < 0.001$). Adults showed lower but non-negligible risks (HI ≤ 0.80), primarily from inhalation during occupational exposure. Importantly,

acidic soils in high-Hg zones accelerate methylmercury formation, creating unquantified dietary exposure pathways. Overall, the results showed that **children face 4-6× higher risk** than adults due to Lower body weight, Higher soil ingestion rates and increased hand-to-mouth behaviour. Supportively, nine of the fifteen (60%) sites exceeded safety thresholds (HI > 1) for children. Additionally, the results showed that Roman Catholic School (Site O, HI = 1.00) and UMaT hostels (Site M, HI = 0.11) show concerning exposure.

Table 6. Pathway-specific Hazard Quotients (HQ) and Hazards Indices at the various sites.

Site	Hg (µg/kg)	Group	CDI_{ing} (mg/kg-day)	CDI_{derm} (mg/kg-day)	CDI_{inh} (mg/kg-day)	HQ_{ing}	HQ_{derm}	HQ_{inh}	HI	Risk Status
A	15,057	Children	1.84×10^{-4}	2.52×10^{-5}	2.32×10^{-5}	3.07	0.42	0.38	**3.87**	High
		Adults	2.16×10^{-5}	3.84×10^{-6}	1.24×10^{-5}	0.36	0.06	0.20	**0.62**	Moderate
B	7,273	Children	8.90×10^{-5}	1.22×10^{-5}	1.12×10^{-5}	1.48	0.20	0.19	**1.87**	High
		Adults	1.04×10^{-5}	1.85×10^{-6}	6.00×10^{-6}	0.17	0.03	0.10	**0.30**	Low
C	8,714	Children	7.42×10^{-5}	1.01×10^{-5}	9.35×10^{-6}	1.24	0.17	0.16	**1.57**	High
		Adults	8.69×10^{-6}	1.54×10^{-6}	5.00×10^{-6}	0.14	0.03	0.08	**0.25**	Low
D	8,774	Children	1.28×10^{-4}	1.75×10^{-5}	1.61×10^{-5}	2.13	0.29	0.27	**2.69**	High
		Adults	1.50×10^{-5}	2.67×10^{-6}	8.63×10^{-6}	0.25	0.04	0.14	**0.43**	Low
E	4,351	Children	6.35×10^{-5}	8.69×10^{-6}	7.99×10^{-6}	1.06	0.14	0.13	**1.33**	High
		Adults	7.44×10^{-6}	1.32×10^{-6}	4.28×10^{-6}	0.12	0.02	0.07	**0.21**	Low
F	2,920	Children	4.00×10^{-5}	5.48×10^{-6}	5.04×10^{-6}	0.67	0.09	0.08	**0.84**	Moderate
		Adults	4.68×10^{-6}	8.32×10^{-7}	2.69×10^{-6}	0.08	0.01	0.04	**0.13**	Low
G	6,320	Children	1.08×10^{-4}	1.48×10^{-5}	1.36×10^{-5}	1.80	0.25	0.23	**2.28**	High
		Adults	1.26×10^{-5}	2.24×10^{-6}	7.26×10^{-6}	0.21	0.04	0.12	**0.37**	Low
H	22,778	Children	2.37×10^{-4}	3.24×10^{-5}	2.98×10^{-5}	3.95	0.54	0.50	**4.99**	High
		Adults	2.78×10^{-5}	4.93×10^{-6}	1.60×10^{-5}	0.46	0.08	0.26	**0.80**	Moderate
I	19,656	Children	1.64×10^{-4}	2.24×10^{-5}	2.06×10^{-5}	2.73	0.37	0.34	**3.44**	High
		Adults	1.92×10^{-5}	3.41×10^{-6}	1.10×10^{-5}	0.32	0.06	0.18	**0.56**	Low
J	7,615	Children	1.02×10^{-4}	1.39×10^{-5}	1.28×10^{-5}	1.70	0.23	0.21	**2.14**	High
		Adults	1.19×10^{-5}	2.12×10^{-6}	6.86×10^{-6}	0.20	0.04	0.11	**0.35**	Low
K	10,065	Children	7.56×10^{-5}	1.03×10^{-5}	9.51×10^{-6}	1.26	0.17	0.16	**1.59**	High
		Adults	8.85×10^{-6}	1.57×10^{-6}	5.09×10^{-6}	0.15	0.03	0.08	**0.26**	Low
L	2,097	Children	1.31×10^{-5}	1.79×10^{-6}	1.65×10^{-6}	0.22	0.03	0.03	**0.28**	Low
		Adults	1.53×10^{-6}	2.72×10^{-7}	8.82×10^{-7}	0.03	0.00	0.01	**0.04**	Low
M	364	Children	5.32×10^{-6}	7.28×10^{-7}	6.69×10^{-7}	0.09	0.01	0.01	**0.11**	Low
		Adults	6.23×10^{-7}	1.11×10^{-7}	3.59×10^{-7}	0.01	0.00	0.01	**0.02**	Low
N	3,695	Children	2.31×10^{-5}	3.16×10^{-6}	2.90×10^{-6}	0.38	0.05	0.05	**0.48**	Low
		Adults	2.70×10^{-6}	4.80×10^{-7}	1.56×10^{-6}	0.05	0.01	0.03	**0.09**	Low
O	2,919	Children	4.76×10^{-5}	6.51×10^{-6}	5.99×10^{-6}	0.79	0.11	0.10	**1.00**	Moderate
		Adults	5.57×10^{-6}	9.89×10^{-7}	3.20×10^{-6}	0.09	0.02	0.05	**0.16**	Low

CDI = Chronic Daily Intake; HQ = Hazard Quotient; HI = Hazard Index (sum of HQs); Risk threshold: HI > 1.0 indicates significant risk.

4. Conclusion

This study integrated geospatial analysis with ecotoxicological and human health risk assessment to unravel mercury (Hg) contamination patterns in Tarkwa-Nsuaem, Ghana. The findings reveal extreme Hg pollution in top soils (364 - 22,778 μg/kg), far exceeding the WHO limit (300 μg/kg), with a distinct NW-SW contamination corridor linked to artisanal and small-scale gold mining (ASGM) activities. Importantly, acidic soils (pH 4.68 - 6.54) in these hotspots amplified Hg mobility, increasing Hg^{2+} solubility and methylmercury formation potential by 60% - 80%. Ecotoxicological risk indices confirmed severe environmental threats, with geoaccumulation indices (I_{geo}: 0.02 - 5.98) classifying fourteen sites as "extremely polluted" and ecological risk indices (ERI: 61 - 3,796) indicating "very high risk" at fourteen sites, where site M near UMaT campus showed moderate risk (ERI = 61) and uncontaminated (I_{geo}: 0.02), aligning with the absence of ASGM activities. Human health risk assessment identified significant non-carcinogenic risks for children (Hazard Index > 1 at nine sites), primarily through soil ingestion. Adults exhibited lower risks but faced unquantified inhalation and dietary threats. Spatial interpolation highlighted a pH-Hg synergy that maximized risks in the central mining belt, particularly near schools and residential clusters. Based on the findings, three remedial actions are recommended (i) liming acidic hotspots (e.g., Site A) to reduce Hg mobility and inhibiting methylmercury formation, (ii) engineered capping of extreme pollution sites (Hg > 15,000 μg/kg) (e.g., Site H [22,778 μg/kg], I [19,656 μg/kg], A [15,057 μg/kg]) to prevent direct soil contact and (iii) limiting agricultural activities in the NW-SW contamination corridor (5.31˚N, 1.99˚W), where there high Hg loading (mean 8,952 μg/kg), acidic soils, and drainage connectivity to the Bonsa River create compounded exposure pathways for crop uptake and aquatic methylation

Further research is recommended for quantifying methylmercury exposure pathways to address the unassessed dietary risks. The studies must prioritize quantifying these vectors through crop/water analysis, human biomonitoring (targeting vulnerable populations), isotopic tracing of methylation hotspots and developing advanced predictive models integrating rainfall patterns and soil pH to quantify dietary risks.

Conflicts of Interest

The authors declare no conflicts of interest regarding the publication of this paper.

References

Adu-Baffour, F., Daum, T., & Birner, R. (2021). Governance Challenges of Small-Scale Gold Mining in Ghana: Insights from a Process Net-Map Study. *Land Use Policy, 102,* Article ID: 105271. https://doi.org/10.1016/j.landusepol.2020.105271

Afrifa, J., Opoku, Y. K., Gyamerah, E. O., Ashiagbor, G., & Sorkpor, R. D. (2019). The Clinical Importance of the Mercury Problem in Artisanal Small-Scale Gold Mining. *Frontiers in Public Health, 7,* Article 131. https://doi.org/10.3389/fpubh.2019.00131

Amuah, E. E. Y., Fei-Baffoe, B., Kazapoe, R. W., Dankwa, P., Okyere, I. K., Sackey, L. N. A. et al. (2024). From the Ground Up: Unveiling Ghana's Soil Quality Crisis and Its Ecological and Health Implications. *Innovation and Green Development, 3,* Article ID: 100097. https://doi.org/10.1016/j.igd.2023.100097

Asamoah, B. D., Asare, A., Okpati, S. W., & Aidoo, P. (2021). Heavy Metal Levels and Their Ecological Risks in Surface Soils at Sunyani Magazine in the Bono Region of Ghana. *Scientific African, 13,* e00937. https://doi.org/10.1016/j.sciaf.2021.e00937

Asare, A., Asamoah, B. D., & Sanful, P. O. (2019). Assessment of Heavy Metal Contaminants Using Pollution Indices in Ankobra River at Prestea Huni-Valley District, Ghana. *Journal of Geoscience and Environment Protection, 7,* 25-35. https://doi.org/10.4236/gep.2019.79003

Ashong, G. W., Kwaansa-Ansah, E. E., Ababio, B. A., Yagra, E. A., & Antwi, G. (2025). Pollution Profiling and Quality Assessment of Bonsa River, Tarkwa Nsuaem, Ghana; Toxic Element, Ecotoxicology, Health Risk Assessment, and Multivariate Analysis. *Environmental Challenges, 18,* Article ID: 101078. https://doi.org/10.1016/j.envc.2024.101078

Birch, G. F. (2003). A Scheme for Assessing Human Impacts on Coastal Aquatic Environments Using Sediments. *Hydrobiologia, 494,* 29-39.

Bortey-Sam, N., Nakayama, S., Akoto, O., Ikenaka, Y., Baidoo, E., Mizukawa, H. et al. (2015). Ecological Risk of Heavy Metals and a Metalloid in Agricultural Soils in Tarkwa, Ghana. *International Journal of Environmental Research and Public Health, 12,* 11448-11465. https://doi.org/10.3390/ijerph120911448

Bravo, A. G., & Cosio, C. (2020). Biotic Formation of Methylmercury: A Bio-Physico-Chemical Conundrum. *Limnology and Oceanography, 65,* 1010-1027. https://doi.org/10.1002/lno.11366

Esdaile, L. J., & Chalker, J. M. (2018). The Mercury Problem in Artisanal and Small-Scale Gold Mining. *Chemistry—A European Journal, 24,* 6905-6916. https://doi.org/10.1002/chem.201704840

Ghana-MIA. (2018). Minamata Convention on Mercury Initial Assessment Report for Ghana (MIA). https://minamataconvention.org/sites/default/files/documents/minamata_initial_assessment/Ghana-MIA-2018.pdf

Gyimah, E., Gyimah, G. N. W., Stemn, E., Ndur, S., Amankwaa, G., & Fosu, S. (2022). Ecological and Human Risk Assessments of Heavy Metal Contamination of Surface Soils of Auto-Mechanic Shops at Bogoso Junction, Tarkwa, Ghana. *Environmental Monitoring and Assessment, 194,* Article No. 830. https://doi.org/10.1007/s10661-022-10429-6

Hakanson, L. (1980). An Ecological Risk Index for aquatic Pollution Control. A Sedimentological Approach. *Water Research, 14,* 975-1001. https://doi.org/10.1016/0043-1354(80)90143-8

Hentschel, T., Hruschka, F., & Priester, M. (2003). *Artisanal and Small-Scale Mining: Challenges and Opportunities.* International Institute for Environment and Development.

Hilson, G. (2003). The Socio-Economic Impacts of Artisanal and Small-Scale Mining in Developing Countries. *Journal of Cleaner Production, 11,* 99-115.

Kamińska, J. A., & Grzywna, A. (2014). Geospatial Interpolation Techniques in Environmental Pollution Mapping. *Journal of Geochemical Exploration, 147,* 120-128.

Kamunda, C., Mathuthu, M., & Madhuku, M. (2016). Health Risk Assessment of Heavy Metals in Soils from Witwatersrand Gold Mining Basin, South Africa. *International Journal of Environmental Research and Public Health, 13,* Article 663.

https://doi.org/10.3390/ijerph13070663

Kumah, R. K (2021). *Ghana Needs to Rethink Its Small-scale Mining Strategy. Here's How.* The Conversation. https://theconversation.com/ghana-needs-to-rethink-its-small-scale-mining-strategy-heres-how-158458

Ministry of Environmental Protection (MEP) & People's Republic of China (2014). *Technical Guidelines for Risk Assessment of Contaminated Sites (HJ 25.3-2014).*

Muller, G. (1969). Index of Geoaccumulation in Sediments of the Rhine River. *Geo Journal, 2,* 108-118.

Osei, L. B., Fosu, S., Ndur, S. A., & Nyarko, S. Y. (2022). Assessing Heavy Metal Contamination and Ecological Risk of Urban Topsoils in Tarkwa, Ghana. *Environmental Monitoring and Assessment, 194,* Article No. 710. https://doi.org/10.1007/s10661-022-10398-w

Owusu, O., Bansah, K. J., & Mensah, A. K. (2019). "Small in Size, but Big in Impact": Socio-Environmental Reforms for Sustainable Artisanal and Small-Scale Mining. *Journal of Sustainable Mining, 18,* 38-44. https://doi.org/10.1016/j.jsm.2019.02.001

Peijnenburg, W. J. G. M., Zablotskaja, M., & Vijver, M. G. (2007). Monitoring Metals in Terrestrial Environments within a Bioavailability Framework and a Focus on Soil Extraction. *Ecotoxicology and Environmental Safety, 67,* 163-179. https://doi.org/10.1016/j.ecoenv.2007.02.008

Quaicoe, I., Beyuo, M., Quaicoe, S., & Lasidzi, N. A. (2023). Diagnostic Gold Deportment Studies and Leaching Behaviour of Small-Scale Gold Mining Tailings from Eastern Region, Ghana. *Journal of Sustainable Mining, 22,* 81-88. https://doi.org/10.46873/2300-3960.1375

Samlafo, V. B., & Ofoe, E. O. (2018). Water Quality Analysis of Bobobo Stream in Tarkwa, Ghana. *Journal of Environmental Hydrology, 8,* 15-19.

Seidu, J., & Ewusi, A. (2018). Assessment of Groundwater Quality Using Hydrogeochemical Indices and Statistical Analysis in the Tarkwa Mining Area of Ghana. *Journal of Environmental Hydrology, 26,* 1-14.

Song, D., Huang, T., Wang, C., Xia, Y., Sun, X., Luo, C. et al. (2025). Transformation of Landfill Leachate into In-Situ Iron-Carbon Galvanic Stabilizer for Effective Remediation of Mercury-Contaminated Soils: A Sustainable Solution. *Environmental Research, 284,* Article ID: 122182. https://doi.org/10.1016/j.envres.2025.122182

US Department of Energy (USDoE) (2011). *The Risk Assessment Information System (RAIS).* Oak Ridge Operations Office. https://rais.ornl.gov/

US Environmental Protection Agency (USEPA) (1989). *Risk Assessment Guidance for Superfund (RAGS), Volume I: Human Health Evaluation Manual (Part A). EPA/540/1-89/002.*

US Environmental Protection Agency (USEPA) (2012). *Integrated Risk Information System (IRIS).* https://www.epa.gov/iris

Wang, Z., Chen, J., Chai, L., Yang, Z., Huang, S., & Zheng, Y. (2011). Environmental Impact and Site-Specific Human Health Risks of Chromium in the Vicinity of a Ferro-Alloy Manufactory, China. *Journal of Hazardous Materials, 190,* 980-985. https://doi.org/10.1016/j.jhazmat.2011.04.039

Wilson, M., Renne, E., Roncoli, C., Agyei-Baffour, P., & Tenkorang, E. (2015). Integrated Assessment of Artisanal and Small-Scale Gold Mining in Ghana—Part 3: Social Sciences and Economics. *International Journal of Environmental Research and Public Health, 12,* 8133-8156. https://doi.org/10.3390/ijerph120708133

World Health Organization (WHO) (2005). *Mercury in Drinking-Water: Background Document for Development of WHO Guidelines.* https://www.who.int/teams/environment-climate-change-and-health/water-sanitation-and-health/chemical-hazards-in-drinking-water

Yu, H., Li, J., & Luan, Y. (2018). Meta-Analysis of Soil Mercury Accumulation by Vegetables. *Scientific Reports, 8,* Article No. 1261. https://doi.org/10.1038/s41598-018-19519-3

Zhang, L. (2017). Heavy Metal Mobility in Acidic Soils: Implications for Environmental Risk Assessment. *Environmental Science & Technology, 51,* 6789-6797.